arXiv:0909.4548v1 [astro-ph.HE] 25 Sep 2009

Unified interpretation of cosmic-ray nuclei and antiproton recent measurements

Giuseppe Di Bernardo[1,2]**, Carmelo Evoli**[3]**, Daniele Gaggero**[1,2]**,
Dario Grasso**[2]**, Luca Maccione**[4]

[1]Dipartimento di Fisica "E. Fermi", Università di Pisa, Largo B. Pontecorvo, 3,
I-56127 Pisa
[2]INFN, Sezione di Pisa, Largo B. Pontecorvo, 3, I-56127 Pisa
[3]SISSA, via Beirut, 2-4, I-34014 Trieste
[4]DESY, Theory Group, Notkestrasse 85, D-22607 Hamburg, Germany

E-mail: `giuseppe.dibernardo@pi.infn.it`, `evoli@sissa.it`,
`daniele.gaggero@pi.infn.it`, `dario.grasso@pi.infn.it`,
`luca.maccione@desy.de`

Abstract. We use our numerical code, DRAGON, to study the implications and the impact of recent CREAM and PAMELA data on our knowledge of the propagation properties of cosmic ray nuclei with energy $\gtrsim 1$ GeV/n in the Galaxy. We will show that B/C (as well as N/O and C/O) and $\bar{p}/p$ data (especially including recent PAMELA results) can consistently be matched within a unique diffusion-reacceleration model. The requirement that light nuclei and $\bar{p}$ data are both reproduced within experimental uncertainties places stringent limits on suitable propagation parameters. In particular, we find the allowed range of the diffusion coefficient spectral index to be $0.38 < \delta < 0.57$ at 95% confidence level and that Kraichnan type diffusion is significantly favored respect to Kolmogorov. While some amount of reacceleration is required to account for low energy data, only a limited range of values of the Alfvèn velocity ($v_A \simeq 15$ km s^{-1}) is allowed. Furthermore, we do not need to introduce any *ad hoc* break in the injection spectrum of primary cosmic rays.

If antiproton data are not used to constrain the propagation parameters, a larger set of models is allowed. In this case, we determine which combinations of the relevant parameters maximize and minimize the antiproton flux under the condition of still fitting light nuclei data at 95% C.L. These models may then be used to constrain a possible extra antiproton component arising from astrophysical or exotic sources (e.g. dark matter annihilation or decay).

1. Introduction

The problems of origin and propagation of Cosmic Rays (CRs) in the Galaxy are long standing questions which need the combination of several different observations in a wide energy range to be answered.

The most realistic description of CR propagation is given by diffusion models. Two main approaches have been developed so far: analytical (or semi-analytical) diffusion
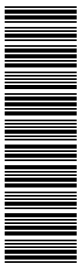
models (see e.g. [1] and ref.s therein), which solve the CR transport equation by assuming simplified distributions for the sources and the interstellar gas, and fully numerical diffusion models. Well known realizations of these two approaches are respectively the *two-zone model* (see e.g. [2, 3, 4]) and the GALPROP package [5, 6, 7]. Recently, some of us developed a new numerical code, DRAGON (Diffusion of cosmic RAys in Galaxy modelizatiON) [8]. All these models involve in general a large number of parameters which need to be fixed using several types of experimental data. Their knowledge is crucial not only for CR physics but also for constraining or determining the properties of an exotic galactic component from indirect measurements.

However, in spite of the strong efforts made on both observational and theoretical sides, most of these parameters are still poorly known. One of the reasons lies in the fact that best quality data on CR spectra (e.g. the ratios of secondary to primary nuclear species) were available mainly at low energy ($E \lesssim 10$ GeV/n), where several competing physical processes (e.g. solar modulation, convection, reacceleration) are expected to affect significantly the CR spectra by an *a priori* undetermined relative amount. Furthermore, the uncertainties on the spallation cross sections and their effects on the propagated CR composition are still sizable at such low energies.

On the other hand, the interpretation of high energy ($E \gtrsim 10$ GeV/n) CR data is, in principle, easier since in this range only spatial diffusion and spallation losses (the latter becoming less and less relevant with increasing energy) are expected to shape the CR spectra. Hence, the study of high energy CR spectra allows in principle to constrain the diffusion properties of CR in the Galaxy, in particular the strength D_0 of the diffusion coefficient at a reference rigidity and its energy slope δ, and offers a lever arm to better understand low energy effects (see [9] for an interesting discussion about this issue). This possibility has been precluded for long time by the scarcity of observational data. The experimental situation however improved recently when the CREAM balloon experiment measured the spectrum of light CR nuclei and especially the boron to carbon ratio (B/C) up to ~ 1 TeV/n [10].

Besides CR nuclear measurements, valuable complementary data were recently provided by the PAMELA satellite experiment which measured the antiproton to proton ratio up to ~ 100 GeV with unprecedented accuracy [11]. As for other secondary nuclear species, antiprotons are expected to be produced by the spallation of primary CRs (mainly protons and Helium nuclei) in the standard scenario. Therefore, their spectrum may provide an independent check of the validity of CR propagation models and a valuable probe of an extra component which may arise, for example, from secondary production in the CR astrophysical sources [12, 13] and/or from dark matter annihilation or decay (see e.g. [14, 15, 16, 17]).

Whether the measured secondary/primary nuclear ratios and antiproton spectra are compatible within the framework of a standard CR transport model is still unclear. Indeed, while a discrepancy between the parameters allowing to reproduce the B/C and the $\bar{p}/p$ was claimed in [18], a good concordance was found in other analyses [14, 19]. Furthermore, the interpretation of nuclear data alone is still confused: analyses based

on the leaky-box and semi-analytical diffusion models favor values of δ significantly larger than the ones found with the numerical GALPROP package. The comparison of such results is not straightforward due to a number of different assumptions. Hence, an independent analysis accounting for most recent available data is timely.

In this work we use DRAGON [8] to constrain the main diffusion parameters against updated experimental data in the energy range $1 \lesssim E \lesssim 10^3$ GeV/n. This code reproduces the results of the well known GALPROP under the same conditions. Furthermore, it allows to test the effects of a spatially varying diffusion coefficient. Here we use the optimized and updated version of this code, which now accounts for ionization and Coulomb energy losses, diffusive reacceleration and convection, and exploits the performances of modern computer clusters to scan a rather large range of parameters. These upgrades allow to constrain the main propagation parameters including the Alfvèn velocity v_A with unprecedented accuracy by means of a statistical analysis of the agreement between model predictions and CR data.

In the following we will present the results of this analysis. In Sec. 2 we briefly review the framework of CR propagation we adopt. In Sec. 3 we describe our analysis and the main results we obtain, while in Sec.s 4 and 5 we compare them with results from other groups and discuss differences and implications for exotic source searches. Section 5 is further devoted to our final remarks and conclusions.

2. The model

Galactic CRs propagate diffusively in the irregular component of the Galactic magnetic field undergoing nuclear interactions with the gas present in the InterStellar Medium (ISM). Similarly to previous treatments, we assume here that CR Galactic source, magnetic field and gas distributions can be approximated to be cylindrically symmetric. Under these conditions CR propagation of stable nuclei in the energy range $1 - 1000$ GeV/n obeys the well known transport equation (Ginzburg and Syrovatskii [20])

$$\frac{\partial N^i}{\partial t} - \boldsymbol{\nabla} \cdot (D \, \boldsymbol{\nabla} - \boldsymbol{v}_c) \, N^i + \frac{\partial}{\partial p} \left(\dot{p} - \frac{p}{3} \boldsymbol{\nabla} \cdot \boldsymbol{v}_c \right) N^i - \frac{\partial}{\partial p} p^2 D_{pp} \frac{\partial}{\partial p} \frac{N^i}{p^2} =$$
$$= Q^i(p, r, z) + \sum_{j>i} c\beta n_{\text{gas}}(r, z)\sigma_{ji}N^j - c\beta n_{\text{gas}}\sigma_{\text{in}}(E_k)N^i . \tag{1}$$

Here $N^i(p, r, z)$ is the number density of the i-th atomic species; p is its momentum; β its velocity in units of the speed of light c; σ_{in} is the total inelastic cross section onto the ISM gas, whose density is n_{gas}; σ_{ij} is the production cross-section of a nuclear species j by the fragmentation of the i-th one; D is the spatial diffusion coefficient; $\boldsymbol{v}_c$ is the convection velocity. The last term on the l.h.s. of Eq. (1) describes diffusive reacceleration of CR in the turbulent galactic magnetic field. In the quasi-liner theory the diffusion coefficient in momentum space D_{pp} is related to the spatial diffusion coefficient by the relationship (see e.g. [1]) $D_{pp} = \dfrac{4}{3\delta(4 - \delta^2)(4 - \delta)} v_A^2 \, p^2/D$ where v_A is the Alfvèn velocity. Here we assume that diffusive reacceleration takes place in the entire diffusive halo.

Although DRAGON allows to account also for CR convection, we neglect this effect in the present analysis showing *a posteriori* that it is not necessary to consistently describe all the available data above 1 GeV/n (see Sec. 4). Hence in the following we will set $\boldsymbol{v}_c \equiv \boldsymbol{0}$.

DRAGON [8] solves Eq. (1) numerically in the stationary limit $\partial N_i / \partial t = 0$ by imposing the following boundary conditions: $N(p, R_{\max}, z) = N(p, r, z_{\min}) = N(p, r, z_{\max}) = 0$, corresponding to free escape of CRs at the outer limit of the Galaxy; a symmetry condition on the axis $r = 0$, $N(p, 0 + \epsilon, z) = N(p, 0 - \epsilon, z)$ ($\epsilon \ll 1$), due to the assumed cylindrically symmetric setup; a null flux condition $\partial N / \partial p = 0$ on the momentum boundaries. The spatial limits of our simulation box are defined by $R_{\max} = 20$ kpc and $z_{\max} = -z_{\min}$. We start the spallation routine from $Z = 16$, having verified that the effect of heavier nuclei on the results of the present analysis is negligible.

We briefly recall below the main assumptions we make for the terms appearing in Eq. (1).

2.1. Spatial diffusion coefficient

The dependence of D on the particle rigidity ρ and on the distance from the Galactic plane z is taken to be

$$D(\rho, r, z) = D_0 \ \beta \left(\frac{\rho}{\rho_0} \right)^{\delta} \quad \exp \left\{ |z| / z_t \right\} \ . \tag{2}$$

As shown in [8], a vertically growing D is physically more realistic than a uniform one and allows to get a more regular behavior of the CR density at the vertical boundaries of the propagation halo with respect to the case of uniform diffusion. For what concerns the analysis discussed in this paper, however, the substitution of such a profile with a vertically uniform D only amounts to a change of the normalization factor D_0. We neglect here a possible dependence on the radial coordinate r, which was considered also in [8]. We always set $z_{\max} = 2 \times z_t$ in Eq. (2) to avoid border effects, and $\rho_0 = 3$ GV in the following. Finally, we assume no break in the power-law dependence of D on rigidity.

2.2. Cosmic ray sources

For the source term we assume the general form

$$Q_i(E_k, r, z) = f_S(r, z) \ q_0^i \ \left(\frac{\rho(E_k)}{\rho_0} \right)^{-\alpha_i} \ , \tag{3}$$

and impose the normalization condition $f_S(r_\odot, z_\odot) = 1$. We assume $f_S(r, z)$ to trace the SNR distribution as modeled in [21] on the basis of pulsar and progenitor star surveys [22]. This is slightly different from the radial distributions adopted in [23] and in [2, 4] which are based on pulsar surveys only. Two-zone models assume a step like dependence of $f_S(r, z)$ as function of z, being 1 in the Galactic disk ($|z| < z_d$) and 0 outside. For each value of δ in Eq. (2) we fix α_i by requiring that at very high energy ($E_k \gg 100$ GeV/n)

the equality $\alpha_i + \delta = \gamma_i$ holds, as expected in a plain diffusion regime. Indeed, at such high energies reacceleration and spallation processes are irrelevant. Here we adopt the same spectral index ($\gamma_i = \gamma$, hence $\alpha_i = \alpha$) for all nuclei as indicated by recent experimental results [24, 25, 26].

The low energy behavior of Q is quite uncertain and several different dependencies of Q on the velocity β have been considered (see e.g. [2]). In the energy range explored in this work, however, different choices of such behavior have negligible effects. This strengthens further the importance of relying on high energy data to reduce systematic uncertainties.

The injection abundances q_0^i are tuned so that the propagated, and modulated, spectra of primary species fit the observed ones. A detailed analysis, accounting for data over the entire rigidity range considered here, will be performed to fix the C, N and O relative source ratios (see below) as these quantities mostly affect the B/C. Rather, the normalization of the source spectra of Oxygen and heavier nuclides is tuned to reproduce the observed spectra in CRs at $E \sim 100$ GeV/n. We verified *a posteriori* that the observed Oxygen spectrum (see below), as well as the subFe/Fe ratios, are reasonably reproduced by our best-fit model.

For the local interstellar spectrum (LIS) of primary protons we adopt $J_p = 1.6 \times 10^4 \, (E_k/1 \text{ GeV})^{-2.73} \, (\text{m}^2 \text{ s sr GeV})^{-1}$ as measured by BESS during the 1998 flight [27]. This spectrum also provides an excellent fit to AMS-01 [28] data and, as we will show below, also to preliminary PAMELA proton spectrum data [29].

What is most important here, however, is that we assume no spectral breaks in the source spectrum of all nuclear species. As we will discuss in Sec. 4 this point is crucial to understand the difference between our results and those of some previous works.

2.3. Nuclear cross sections

The spallation cross sections and the spallation network are based on a compilation of experimental data and semi-empirical energy dependent interpolation formulas as provided e.g. in [30, 31, 32] (see also GALPROP, [7] and references therein).

For antiprotons, the main processes responsible for their production are $p - p_{\text{gas}}$, $p - \text{He}_{\text{gas}}$, $\text{He} - p_{\text{gas}}$ and $\text{He} - \text{He}_{\text{gas}}$ reactions, plus a negligible contribution from other nuclei. Similarly to [18, 19] we adopt the $\bar{p}$ production cross-section calculated using the parametrization given in Tan & Ng [33]. Inelastic scattering, annihilation and tertiary $\bar{p}$ (antiprotons which have been inelastically scattered) are treated as in [18].

2.4. Target gas

The ISM gas is composed mainly by molecular, atomic and ionized hydrogen (respectively, H_2, HI and HII). Here we adopt the same distributions as in [5, 8]. We checked that other possible choices do not affect significantly our final results.

Following [34] we take the He/H numerical fraction in the ISM to be 0.11. We neglect heavier nuclear species.

2.5. Solar modulation

We describe the effect of solar modulation on CR spectra by exploiting the widely used force-free approximation [35], prescribing that the modulated spectrum $J(E_k, Z, A)$ of a CR species is given, with respect to the Local Interstellar Spectrum (LIS) $J_{\text{LIS}}(E_k, Z, A)$, by

$$J(E_k, Z, A) = \frac{(E_k + m)^2 - m^2}{\left(E_k + m + \frac{Ze}{A}\Phi\right)^2 - m^2} \, J_{\text{LIS}}\left(E_k + \frac{Ze}{A}\Phi, Z, A\right), \tag{4}$$

where m is the nucleon mass and Φ is the so called modulation potential. This potential is known to change with the solar activity with a period of 11 years and to change polarity with a period twice longer. It must be stressed that the potential Φ is not a model independent quantity. Rather, for each propagation model it should be obtained by fitting the CR spectra at low energy. The possibility of restricting our analysis to $E_k > 1$ GeV/n will reduce the systematic uncertainties associated to this unknown. Above 1 GeV/n the effects of modulation on the secondary/primary CR ratios used in our analysis are tiny and can safely be accounted for by means of the simple force free approximation.

For protons and antiprotons we use $\Phi = 700$ MV which allows to match BESS98 [27], AMS-01[28] and PAMELA [29] proton data even well below 1 GeV/n (see Fig. 5(e)). Indeed all these experiments took their data in a period with almost the same, almost minimal, solar activity. For secondary/primary light nuclei ratios we use $\Phi = 650$ MV which allows us to best reproduce Oxygen taken by ACE/CRIS [36] data taken also near solar minimum. We verified that changing Φ within a reasonable interval do not affect significantly the final results of our analysis.

3. Analysis and results

Our goal is to constrain the main propagation parameters δ, D_0, z_t and v_A entering Eq. (2). To this aim, we compare to experimental data our prediction for the following physical quantities: the B/C, N/O, C/O ratios for $1 < E_k < 10^3$ GeV/n and the $\bar{p}/p$ ratio for $1 < E_k < 10^2$ GeV/n. We will check *a posteriori* that also the Oxygen, proton and antiproton absolute spectra are correctly reproduced by our preferred models.

As long as the propagation halo scale height is allowed to vary within the range $2 \lesssim z_t \lesssim 6$ kpc (which is what we assume here), D_0 and z_t are practically degenerate so that our results depend only on the ratio D_0/z_t. Throughout this paper we will always express this quantity in units of 10^{28} cm^2 s^{-1} kpc^{-1}. We verified *a posteriori* that for this range of z_t values, the predicted ^{10}Be/^{9}Be ratio, which constrains the CR propagation time hence the vertical scale height of the propagation region [1] when combined with secondary/primary stable nuclei data, is consistent with experimental data.

3.1. Light nuclei ratios

3.1.1. Method We already showed [8] that in order to constrain correctly the propagation parameters on the basis of B/C measurements it is essential to take into proper account that the primary parent species of Boron are also affected by propagation. This holds not only for the Nitrogen ($N = {}^{14}N + {}^{15}N$), which gets a significant secondary contribution, but also for Carbon and Oxygen, since for $E_k < 100$ GeV/n their spectra are shaped by spallation losses in a propagation dependent way. Therefore, we perform our likelihood analysis in three steps:

(i) for fixed values of the propagation parameters v_A, δ, and D_0/z_t we vary the C/O and N/O source ratios to compute the χ^2‡ (which we call $\chi^2_{C,N,O}$) of the propagated, and modulated, C/O and N/O ratios against experimental data in the energy range $1 < E_k < 10^3$ GeV/n;

(ii) for the same fixed value of v_A, we finely sample the parameter space (δ, D_0/z_t) by using, for each couple of these parameters, the C/O and N/O source ratios which minimize $\chi^2_{C,N,O}$; for each of these realizations we compute the χ^2 (which we call $\chi^2_{B/C}$) for the B/C modulated ratio against data in several energy ranges;

(iii) we repeat the same analysis for several values of v_A to probe the effect of diffusive reacceleration. For each value of v_A we then determine the allowed ranges of δ and D_0/z_t for several Confidence Levels (CL).

In [8] only items (i) and (ii) were performed, for $v_A = 0$ and without accounting for CREAM data, not yet public at that time.

Here, besides CREAM's, we use experimental data provided by the HEAO-3 [38] and CRN [40] satellite-based experiments. HEAO-3 B/C data are nicely confirmed from a recent preliminary analysis of AMS-01 data [39] which, however, we do not use in our work.

The wide energy range covered by these data allows us to perform our analysis using three different energy intervals defined by $E_{\min} = 1$, 5 and 10 GeV/n respectively and by the same $E_{\max} = 1$ TeV/n. This procedure allows us to better probe the effects of reacceleration and to test the possible relevance of other unknown low energy physics.

3.1.2. Results In Tab. 1 we report the best-fit model parameters, and the relative minimal $\chi^2_{B/C}$'s, as determined for several values of v_A and $E_{\min}$. Confidence regions in the plane ($D_0/z_t, \delta$) are shown in Fig. 1 for several values of v_A and $E_{\min} = 1$ GeV/n.

First of all we notice that in the highest energy range ($E_{\min} = 10$ GeV/n) the best-fit model values of δ and D_0/z_t are weakly dependent on the Alfvèn velocity. In particular, the best fit values of δ fluctuates within the very narrow range $0.41 \div 0.46$ varying v_A in the range $0 \div 30$ km/s. This agrees with the common wisdom that reacceleration is almost ineffective at such high energies. Therefore, the analysis performed for $E_{\min} = 10$ GeV/n

---

‡ Every time we refer to a χ^2, we mean the χ^2 divided by the number of degrees of freedom, i.e. the so called reduced χ^2.

Table 1. Best fit parameter resulting from comparing our model prediction with B/C experimental data (B/C analysis) and with B/C and $\bar{p}/p$ experimental data (combined statistical analysis), as described in text.

		B/C analysis			joint analysis		
v_A [km/s]	E_{min} [GeV/n]	δ	D_0/z_t	χ^2	δ	D_0/z_t	χ^2
0	1	0.57	0.60	0.38	0.49	0.79	1.63
	5	0.49	0.68	0.38	0.49	0.96	0.85
	10	0.46	0.73	0.19	0.55	0.90	1.63
10	1	0.52	0.68	0.32	0.49	0.79	0.87
	5	0.46	0.73	0.40	0.52	0.90	1.92
	10	0.44	0.79	0.19	0.60	0.79	3.46
15	1	**0.46**	**0.76**	0.33	0.49	0.79	0.87
	5	0.44	0.79	0.36	0.52	0.90	1.92
	10	0.44	0.82	0.20	0.60	0.79	3.46
20	1	0.41	0.90	0.47	0.41	1.01	1.92
	5	0.46	0.79	0.29	0.49	0.98	1.09
	10	0.41	0.87	0.21	0.52	0.98	1.91
30	1	0.33	1.20	0.40	0.41	1.01	1.92
	5	0.38	1.04	0.19	0.49	0.98	1.09
	10	0.41	0.95	0.16	0.52	0.98	1.91

best probes indeed the actual physical values of δ and D_0/z_t. On the other hand, when also lower energy data are taken into account, reacceleration plays a relevant role, as demonstrated by the strong dependence of these parameters on v_A for the case $E_{min} = 1$ GeV/n. In that case, the minimal χ^2's correspond to $v_A = 10$, 15 km/s. The latter value has to be preferred because of the lower χ^2 at intermediate energies ($E_{min} = 5$ GeV/n) and because the best-fit values of δ and D_0/z_t are almost independent on E_{min}, as expected if all relevant physics were taken into account.

Our preferred set of parameters is therefore $v_A = 15$ km/s and $(\delta, D_0/z_t) = (0.45, 0.8)$ (due to the large errors involved in this analysis, the small variations of the best values with E_{min} are irrelevant and the last digits of their value have been approximated).

We show in Fig. 2(a) to 2(c) that for this choice of the parameters the B/C and N/O and C/O data are all nicely reproduced. In the same figures we also show the effect of varying v_A by keeping fixed δ and D_0/z_t to their best-fit values. Again, the best match with data is achieved with $v_A = 15$ km/s. It should be noted that C/O CREAM data points differ significantly from those of the other experiments for $E_k > 10$ GeV/n. Due to their large statistical errors, however, these data have almost no effects on the results of our analysis. The best fit value of the N/O source abundance is 6 % which is in good agreement with previous results based on low energy data [37]. As a consistency check, in Fig. 2(d) we show that the absolute Oxygen spectrum computed with our preferred
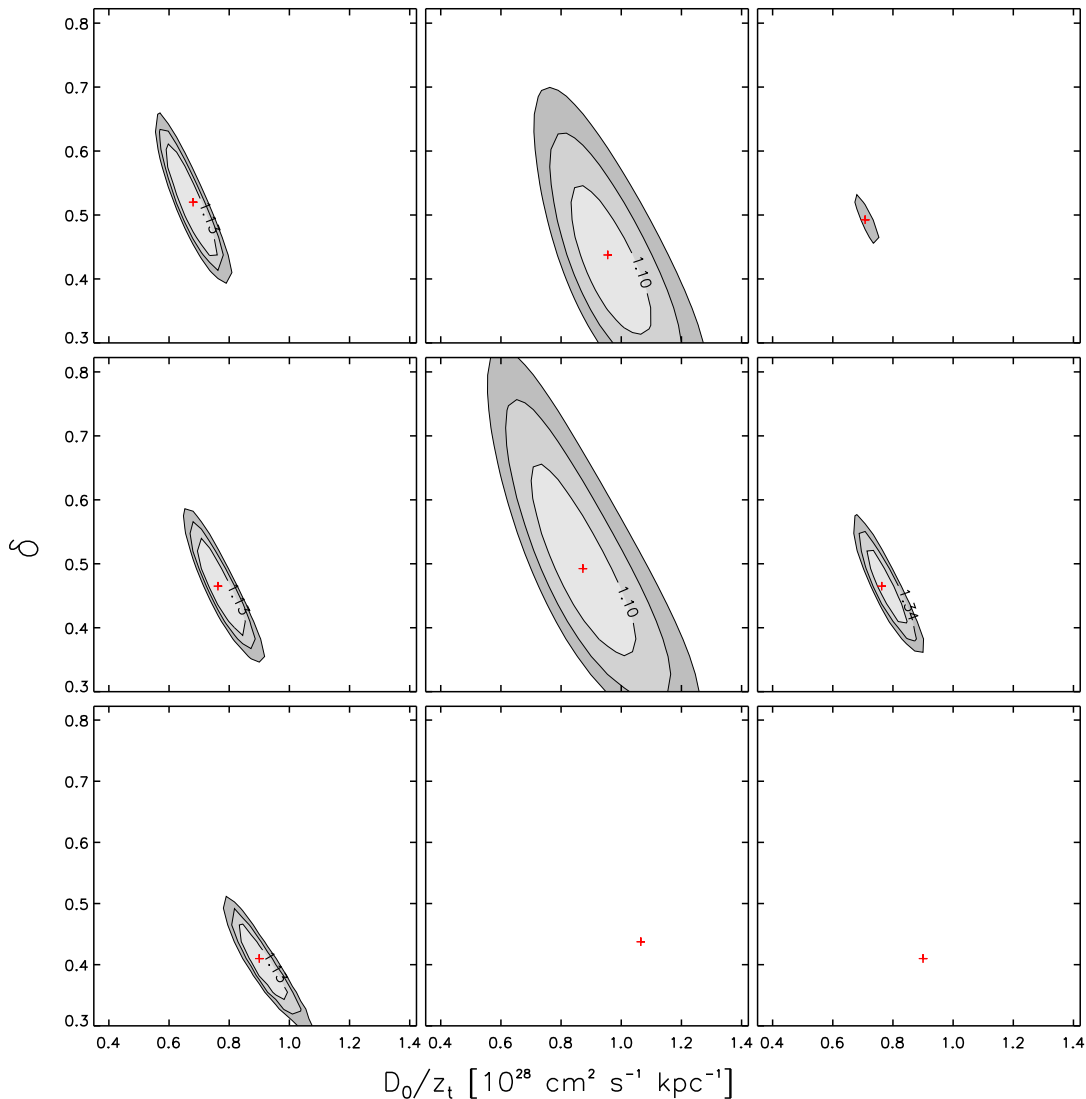
Figure 1. The 68%, 95% and 99% confidence level regions of DRAGON models, computed for $E_{\min} = 1$ GeV/n are represented in the plane $(D_0/z_t, \delta)$. For the 68% confidence level the corresponding value of the χ^2 is also shown. The red crosses show the best-fit position. Each row corresponds to different values of the Alfvèn velocity: $v_A = 10, 15, 20$ km/s from top to bottom. Each column corresponds to different analyses: B/C (left panels), $\bar{p}/p$ (center panels) and combined (right panels).

model is also in reasonably good agreement with experimental data.

We would like to stress here that although the results obtained in this section favor $v_A \simeq 15$ km/s and $\delta \simeq 0.45$, other combinations of parameters, as those shown in Tab. 1, have acceptable $\chi^2_{\mathrm{B/C}}$ and cannot therefore be excluded on the basis of light nuclei secondary/primary data alone. For example, a model with $v_A = 30$ km/s and $\delta = 0.33$, has a minimal $\chi^2_{\mathrm{B/C}} = 0.40$ and indeed provides an acceptable description of the experimental data (see Sec. 4). The CL regions shown in Fig. 1 provide a graphical representation of the statistical uncertainties on the determination of δ and D_0/z_t for
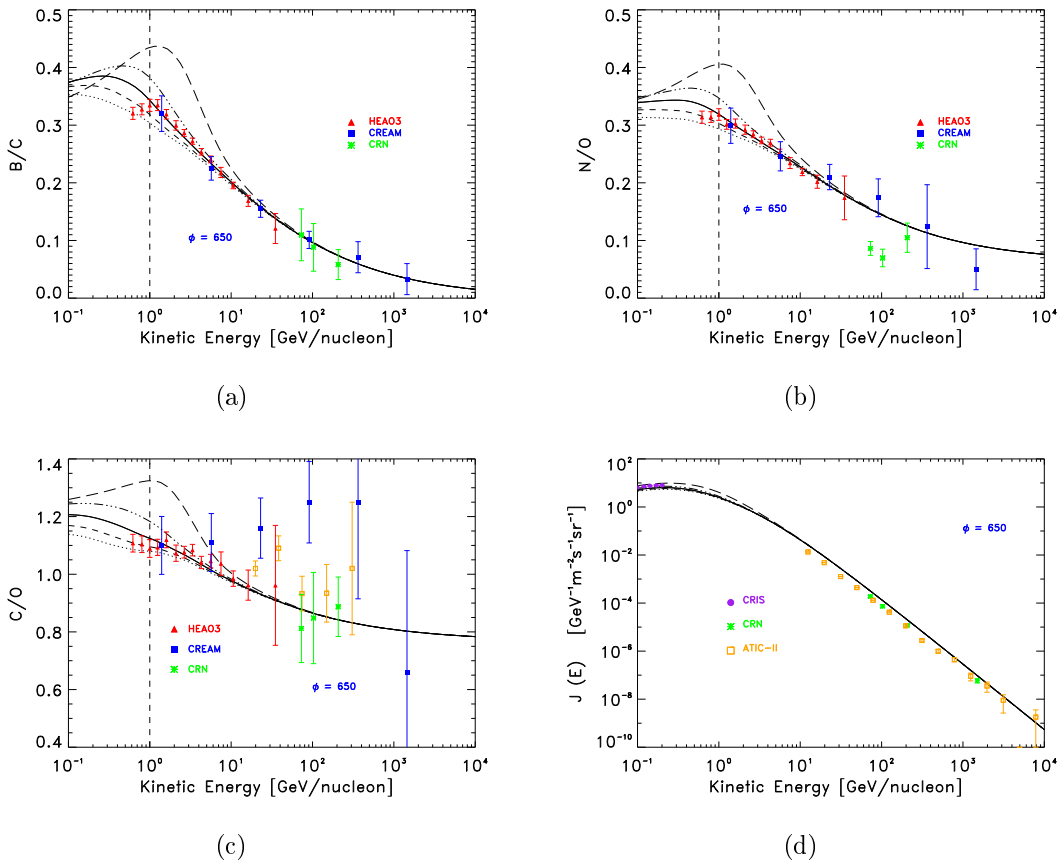
Figure 2. The B/C (panel a), N/O (panel b), and C/O (panel c) ratios and the Oxygen spectrum (panel d) as obtained with DRAGON for $\delta = 0.45$ and $D_0/z_t = 0.8$ are plotted for several values of v_A and compared with the respective experimental data. Dotted, short-dashed, solid, dot-dashed, long-dashed correspond to $v_A = 0, 10, 15, 20, 30$ km/s respectively. A modulation potential $\Phi = 650$ MV has been adopted, as it allows to best reproduce low energy Oxygen data.

each considered value of v_A.

In the next section we will show how the $\bar{p}/p$ and absolute proton spectra measurements offer a powerful tool to further constrain allowed propagation models.

3.2. Antiprotons

3.2.1. Method The statistical analysis for the $\bar{p}/p$ ratio is rather simpler than the one for B/C. Indeed, the secondary $\bar{p}$ production depends, besides on D_0/z_t, δ and v_A, only on the source abundance ratio He/p. This last unknown quantity can be easily fixed by looking at the measured spectrum of He at Earth, which is relatively well known. Therefore, we do not need to fit the source abundance ratio here and can directly proceed to map the $\chi^2_{\bar{p}/p}$ in the $(D_0/z_t,\ \delta)$ space, for several v_A, similarly to what described in items (ii) and (iii) of the previous subsection.

(a)

(b)

(c)
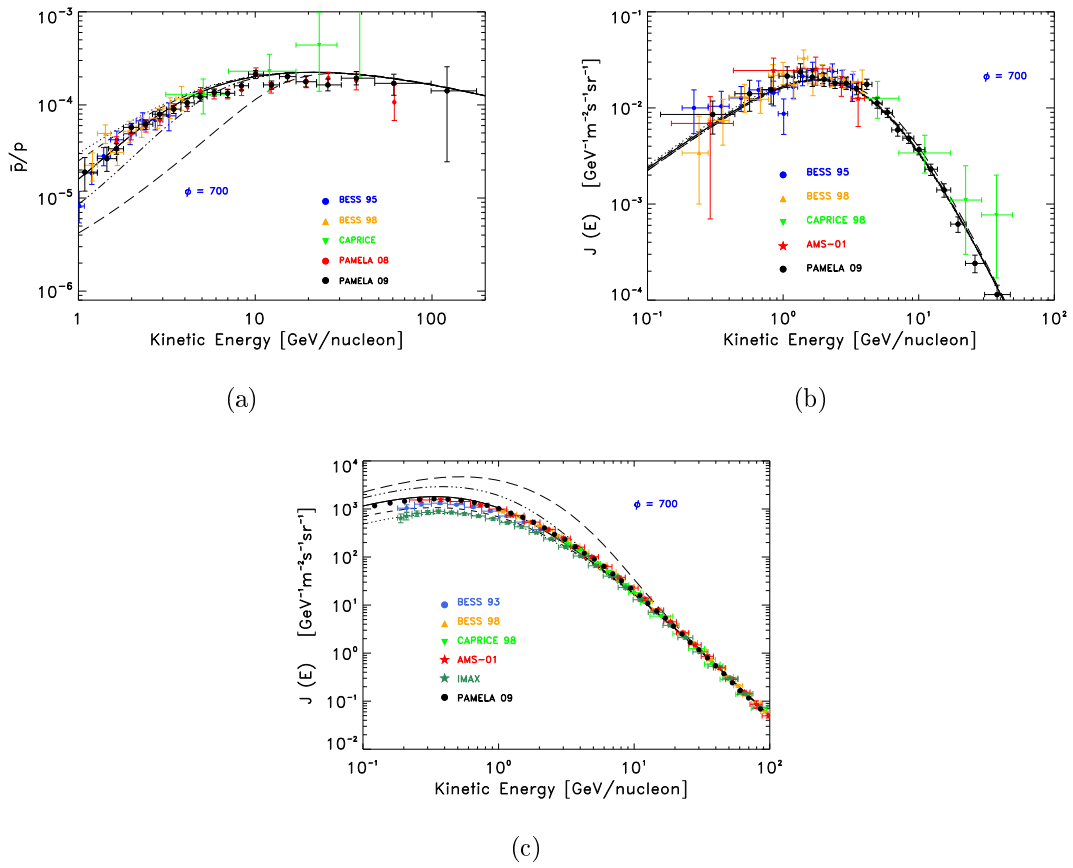
Figure 3. The antiproton to proton ratio (panel a), the antiproton spectrum (panel b) and the proton spectrum (panel c) as obtained with DRAGON for $\delta = 0.44$ and $D_0/z_t = 0.8$ are plotted for several values of v_A and compared with experimental data. The dotted, short dashed, solid, dot-dashed and long dashed curves correspond to $v_A = 0, 10, 15, 20, 30$ km/s respectively. The force-free field potential $\Phi = 700$ MV is adopted to modulate our theoretical model spectra, as it gives the best match to proton data.

3.2.2. Results In the second column of Fig. 1 we show the statistically allowed regions in the plane $(D_0/z_t, \delta)$ for several values of v_A and compare them with the corresponding regions determined from the light nuclei analysis (first column in the same figure). Noticeably, the results of the $\bar{p}/p$ analysis depend strongly on the value of v_A. If no break in the proton source spectrum is introduced, large values of v_A are disfavored, with $v_A \geq 20$ km/s being excluded at 99 % CL. We will show that this effect is mainly driven by the strong dependence of the proton spectrum on reacceleration at low energies.

The parameter regions constrained by the B/C and $\bar{p}/p$ data for $v_A = 15$ km/s overlap quite nicely. Indeed, the preferred model found on the basis of the light nuclei analysis provides also an excellent fit of $\bar{p}/p$ data, updated with the last PAMELA release (see Fig. 3(a)). Such a concordance is one of the main results of this work. As we did in Fig. 2(a) for the B/C, in Fig. 3(a) we show the effect of varying v_A on the $\bar{p}/p$ ratio, with δ and D_0/z_t being fixed.

It is also useful to compare DRAGON predictions with the antiproton absolute flux measurements. Again, we see from Fig. 3(b) as our light nuclei preferred model provides an excellent fit of available data. It is noticeable, however, that for fixed δ and D_0/z_t the antiproton absolute flux is almost independent of v_A, meaning that the effect of reacceleration on the $\bar{p}/p$ is driven by that on protons, as evident in Fig. 3(c).

Dealing with the $\bar{p}/p$ data in our likelihood analysis, we need to verify that the observed proton spectrum is also correctly reproduced by our preferred model. In Fig. 3(c) we show this to be the case even down to energies $\lesssim 1$ GeV. We notice that large values of v_A do not reproduce the proton spectrum. We use here the force-free field modulation potential $\Phi = 700$ MV, which is not too far from what was done in previous analyses (see e.g. [6]). This choice best matches BESS98 [27] and AMS-01 [28] proton data and noticeably also PAMELA proton preliminary data [29].

3.3. Combined analysis and constraints on the propagation parameters

A combined analysis of light secondary/primary nuclei and antiproton/proton data can be performed under the working hypothesis that CR antiprotons are only of secondary origin.

We define the combined reduced χ^2 as $\chi^2_{\text{comb}} = \frac{1}{2}\left(\chi^2_{\text{BC}} + \chi^2_{\text{ap/p}}\right)$. The CL regions for several values of v_A are reported in the third column of Fig. 1 and the corresponding best-fit parameters in Tab. 1. As we anticipated in the previous subsection, large values of v_A were already excluded by the $\bar{p}/p$ data alone. Here we see that even for the allowed values of v_A, the parameter region constrained by the light nuclei analysis narrows significantly when $\bar{p}/p$ is taken into account.

Indeed, among the values considered in our analysis only $v_A = 15$ km/s is allowed at 2σ. For this value of v_A the 95% CL allowed ranges of the other propagation parameters are $0.38 < \delta < 0.57$ and $0.63 < D_0/z_t < 0.73$ with best-fit at $(\delta, D_0/z_t) = (0.47, 0.76)$, practically coinciding with the result of the light nuclei analysis alone.

It should be mentioned that our analysis accounts only for statistical experimental errors as the effect of systematic errors in different data sets can hardly be reliably estimated. It worth noticing that the uncertainties on same of the particle physics (spallation cross sections) and astrophysical parameters may also slightly weaken our constraints on the propagation models.

3.4. Maximal and minimal antiproton spectra

The previous results clearly favor a standard interpretation of the measured antiproton spectrum in terms of purely secondary production from CR nuclei. It is still possible, however, that a subdominant antiproton component arises from unconventional processes. In order to constrain such "exotic" component(s) with experimental data, one has to compare these data with the predictions of the theoretical models validated against CR nuclei data alone.
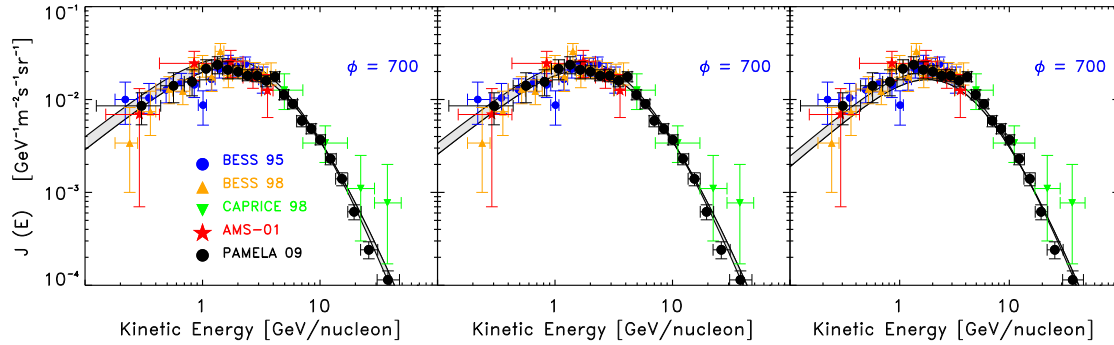
Figure 4. The $\bar{p}$ absolute spectrum is shown for $v_A = 0, 10, 20$ (from the left to the right panels respectively). The upper and lower curves correspond to the MAX and MIN models defined as in Sec. 3.4 respectively.

For this purpose we define, for each value of v_A considered in the above, a pair of MAX and MIN models which maximize and minimize respectively the antiproton absolute flux integrated in the range $1 - 100$ GeV under the condition to be compatible with secondary/primary light nuclei data down to 1 GeV/n within 95% CL.

In Fig. 4 we show the allowed ranges of the antiproton absolute spectrum for several values of v_A. Among the models considered here the absolute MAX and MIN models are those defined by the parameters $(\delta, D_0/z_t, v_A) = (0.63, 0.57, 10)$ and $(0.30, 1.28, 30)$ respectively. Therefore, we conclude that, under the hypotheses adopted in this work, $\bar{p}$ constraints on an exotic component should not use, as propagation models, any model whose $\bar{p}$ background prediction is lower than our MIN (or larger than our MAX) model, as it would be in contrast with B/C data at 95% CL. Hence, the most conservative constraint, under our hypotheses, arises from the request that the sum of the background $\bar{p}$ predicted by the MIN model plus the exotic $\bar{p}$ component do not exceed the experimental data, within some CL.

4. Discussion and comparison with previous results

As we mentioned above, our numerical diffusion code DRAGON reproduces the same results of GALPROP under the same physical conditions. Our analysis and main conclusions, however, differ significantly from those reported in several papers based on that code.

In order to clarify the reasons of such a discrepancy, in Fig. 5(a) and 5(c) we compare the predictions of our preferred model $(\delta, D_0/z_t, v_A) = (0.45, 0.8, 15)$ with those of two models adopting the same propagation parameters (and source distribution) as the "conventional GALPROP model" discussed in [6], namely $(\delta, D_0(4 \text{ GV})/z_t, v_A) = (0.33, 1.45, 30)\S$. These last models, represented by the solid/dashed red lines, differ for

§ GALPROP uses a spatially uniform diffusion coefficient, hence $z_t = z_{\max} = 4$ kpc in this case. As we already noticed, for the purposes of the present analysis adopting a vertically uniform or varying diffusion coefficient only amounts to a rescaling of D_0/z_t. We verified that this does not affect any

the presence/absence of a break at $\rho_{\text{break}} = 9$ GV in the CR nuclei source spectra. Such spectral feature was adopted in [6], in order to reproduce low energy data. Indeed we see from Fig. 5(e) that if no break is assumed, the proton spectrum and, as a consequence, also the $\bar{p}/p$ ratio computed with the conventional GALPROP model parameters are in contrast with low energy data.

While below 1 GeV/n the "conventional GALPROP model" provides a better description of the observed B/C, above this reference energy, hence from 1 to 10^3 GeV/n, all data sets are best described by our model, with no need of invoking a (hardly justifiable) break in the injection spectrum at 9 GV. CREAM B/C data favor a value of δ larger than 0.33, which also allows a much better fit of N/O HEAO-3 [38] data if no break is assumed (see Fig. 5(b)). However, while light nuclei data alone do not allow further discriminations between models, what most favor our preferred model are BESS [27], CAPRICE [41] and especially the preliminary PAMELA measurements of the antiproton absolute spectrum [29]. Indeed, the discrepancy between low energy antiproton data and the prediction of the "conventional GALPROP model", which was already noted in [6], becomes more compelling due to the new PAMELA data, as shown in Fig. 5(d). Furthermore, the source spectral break does not affect the absolute $\bar{p}$ spectrum and therefore does not help ameliorate that discrepancy.

As we discussed in the introduction, the B/C excess in the prediction of our preferred model below 1 GeV/n can be due to a number of reasons. For example, it was shown that the dissipation of magneto-hydrodynamics waves in the ISM due to their resonant interaction with CRs may favor the escape of low energy primary species so to explain the observed peak at ~ 1 GeV/n [42]. Interestingly, the preferred value of δ found with GALPROP in that case is 0.5 which almost agrees with the result of our analysis (although a break in the injection index was still invoked in that work).

The comparison of our results with those of semi-analytical models is more difficult for obvious reasons. One of the difficulties lies in the simplified gas and source distribution adopted in those models (see Sec. 2). We verified, however, that such differences only affect the constraints to D_0/z_t with almost no effect on the determination of δ. We also need to take into account that semi-analytical models (see e.g. [2, 3]) often assume that diffusive reacceleration takes place only in the thin Galactic disk, while in the numerical models, as the one presented here, it takes place in the entire diffusion halo. Therefore, in order to compare the value of the Alfvèn velocity estimated in those works with ours it is necessary to perform a proper rescaling. This is approximatively given by (see e.g. Eq. (18) in [4]) $v_A = v_A^{\text{SA}} \sqrt{z_d/z_t}$, with v_A^{SA} being the Alfvèn velocity in the semi-analytical models and z_t the half scale height of the Galactic disk.

In spite of these differences, and that CREAM and PAMELA data were not included in those analyses for chronological reasons, it is comforting that for low values of the convective velocity $v_c \simeq 0$ the preferred value of δ estimated in [2, 3] is in remarkably good agreement with that found in this work: $\delta \simeq 0.46$. Interestingly, the rescaled value

other result of our analysis.

(a)

(b)

(c)

(d)

(e)
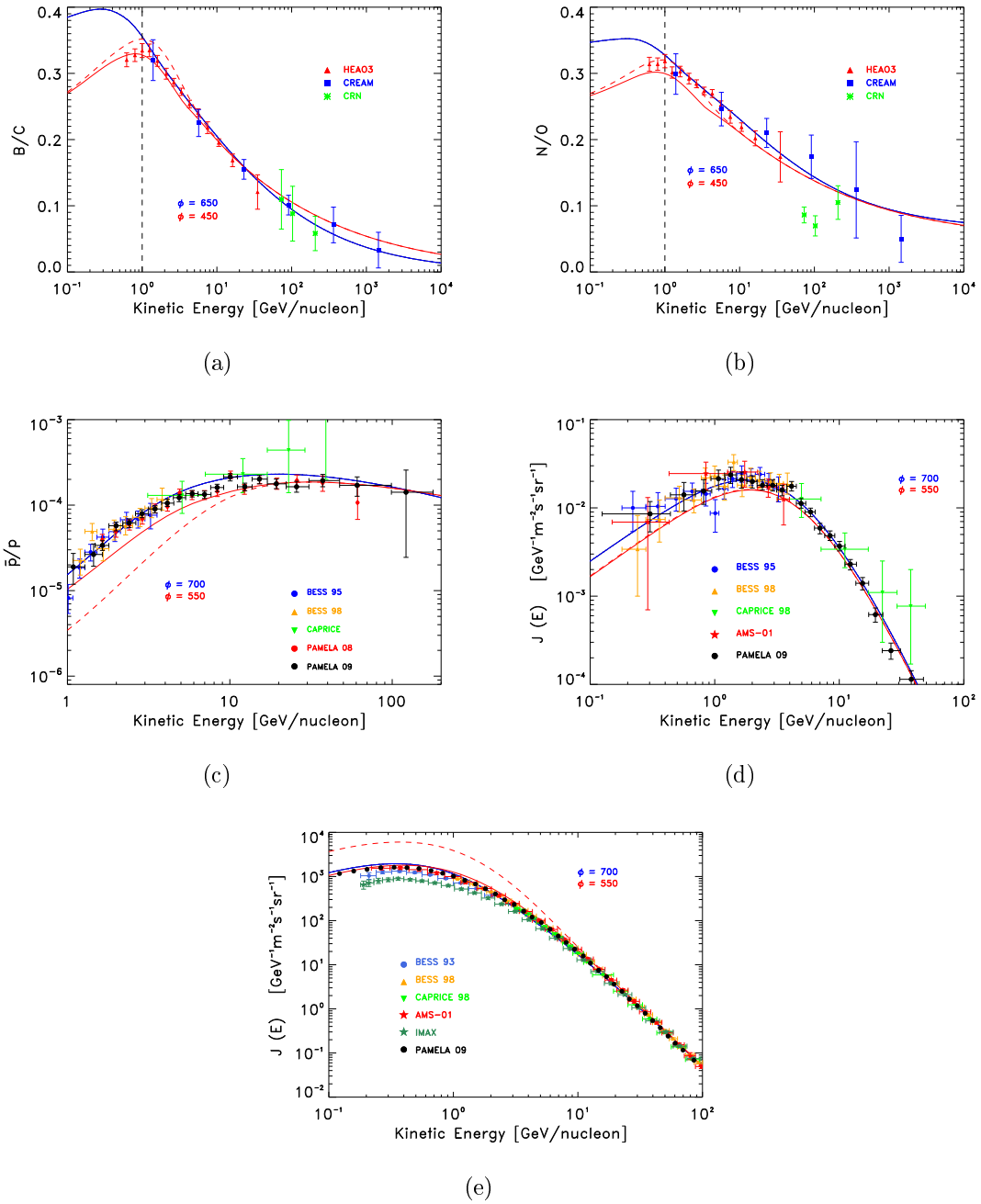
Figure 5. The B/C (panel a), N/O (panel b), $\bar{p}/p$ (panel c), $\bar{p}$ (panel d) and proton (panel e) spectra computed with our preferred model (blue solid line), the "conventional" GALPROP reference model (red solid line) and the same model with no break in the CR source spectrum (red dashed line), are compared with available experimental data. In both cases we use DRAGON to model CR propagation and interactions. Here we use $\Phi = 550$ MV to modulate the "conventional GALPROP model" and $\Phi = 700$ MV to modulate our model, since such potentials allow the best fit of proton AMS01 [28], BESS98 [27] and PAMELA data [11, 29] at low energy for the two models respectively.

(a)   (b)
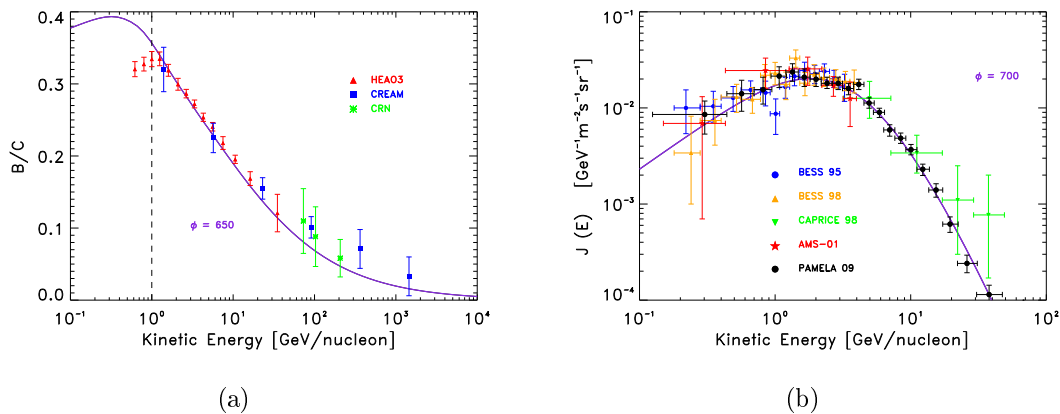
Figure 6. The B/C ratio (panel a) and $\bar{p}$ flux (panel b) are shown for the following choice of the propagation parameters: $\delta = 0.6$, $D0/z_t = 0.6$, $v_A = 15$ and $v_c = 10$.

of v_A determined in [2] for $v_c \simeq 0$ is $v_A \simeq 10$ which is also in good agreement with our results. It is important to notice that, similarly to what we did in our analysis, no break in the source spectral index was assumed in [2, 3]. We remind the reader that in the above we always assumed $v_c = 0$ as higher values of that parameter are not required to interpret CR nuclei and antiproton data for $E_k > 1$ GeV/n, while the analysis performed in [2, 3] accounts also for data down to 0.6 GeV/n. We tested, however, how a non-vanishing convective velocity (taken to be uniform in the diffuse halo for simplicity) affects our results. In agreement with [2, 3], we found that for $v_c \simeq 10$ km s^{-1} HEAO-3 light nuclei data above 1 GeV/n can be reproduced by models with $\delta \simeq 0.6$. In that case, however, the fit of high energy B/C CREAM data becomes significantly worse (see Fig. 6(a)), while PAMELA $\bar{p}$ flux data are still nicely reproduced (see Fig. 6(b)).

Several semi-analytical two-zone models were found to provide a good combined fit to the B/C and antiproton data (see e.g. [19, 4]). Unfortunately, among the models reported in the literature we did not find one with parameters corresponding to our best fit model, so that a direct comparison with our results is not possible here.

Respect to the results of our previous analysis reported in [8], where the numerical and statistical methods followed here where first discussed but which did not account for CR reacceleration and for CREAM and PAMELA data, we get here almost consistent results in the case $v_A = 0$.

5. Conclusions

We used recent data on CR light nuclei and antiprotons to determine the conditions of propagation of high energy CRs in the Galaxy, exploiting our numerical code, DRAGON. In the framework of a diffusion-reacceleration model, we performed a thorough analysis of the agreement of our predictions with experimental information, aimed at constraining, in a statistical sense, the most important model parameters: D_0/z_t, δ and v_A. The amount and quality of data is enough to allow us to restrict

our analysis to energies above 1 GeV/n, and also to check the evolution of our results varying the minimal energy at which data are considered. This is essential to reduce the uncertainties related to possibly unknown low energy physics, including solar modulation, and to disentangle the effects of reacceleration from those of diffusion.

The most important result of this analysis is that light nuclei (especially B/C) data and antiproton data above 1 GeV/n can be fit into a unique, coherent model of propagation, as it can be read off Fig. 1. Indeed, the confidence regions of the light nuclei and antiproton independent analyses nicely overlap to produce combined constraints on D_0/z_t, δ and v_A. Interestingly, while the constraint on the diffusion parameters is placed mainly by light nuclei data, proton and antiproton data help constraining v_A, disfavoring large values of the Alfvèn velocity ($\gtrsim$ 20 km/s). In particular, only $v_A \simeq 15$ km/s is allowed. For this value of the Alfvèn velocity, the range of the other parameters, allowed at 95% CL, are $0.38 < \delta < 0.57$ and $0.63 < D_0/z_t < 0.73$, with best-fit at $(\delta, D_0/z_t) = (0.47, 0.76)$ (we remind the reader that D_0/z_t is expressed here in units of 10^{28} cm^2 s^{-1} kpc^{-1} and v_A in km s^{-1}). We also found that the preferred value of the N/O ratio at injection is $\sim$ 6 %. These results, and in particular the analysis of data with $E_{min} = 10$ GeV/n, seem to favor a Kraichnan spectrum ($\delta = 0.5$) for the magnetic turbulence in the Galaxy. It worth noticing that a relatively large value of δ, as that preferred by our analysis, would give rise to a too large CR anisotropy if our results are extrapolated to $E_k \gg 10^{14}$ eV/n (see e.g. [43] and ref.s therein). Our results, therefore, may imply some change in the CR propagation properties at very high energy and call for a more complex picture.

Given that anyway nuclei data alone are able to provide constraints on D_0/z_t and δ, we use this information to establish a range for the maximal and minimal flux of antiprotons expected from CR interactions in the gas and still compatible with light nuclei observations within 95% CL. This range information can be used as a CR background in analyses aimed at constraining or finding some exotic signal in antiproton data.

Forthcoming data from several running or scheduled experiments, as PAMELA (both for antiprotons and light nuclei), CREAM-II [24], TRACER [25, 26], and especially AMS-02 [44] which will measure both CR nuclei and $\bar{p}$ fluxes from hundreds MeV/n up to TeV/n, will soon allow tighter constraints.

Acknowledgments

References

[1] Berezinsky V S *et al.*, Astrophysics of Cosmic Rays, North-Holland, 1990
[2] Maurin D, Donato F, Taillet R and Salati P, 2001 *Astrophys. J.* **555** 585 [arXiv:astro-ph/0101231]
[3] Maurin D, Taillet R and Donato F, 2002 *Astron. Astrophys.* **394** 1039 [arXiv:astro-ph/0206286]
[4] Maurin D *et al.*, [arXiv:astro-ph/0212111]
[5] Strong A W and Moskalenko I W, 1998 *Astrophys. J.* **509** 212 [arXiv:astro-ph/9807150]
[6] Strong A W, Moskalenko I V and Reimer O, 2004 *Astrophys. J.* **613** 962 [arXiv:astro-ph/0406254]
[7] GALPROP project web page: http://galprop.stanford.edu/web_galprop/galprop_home.html
[8] Evoli C, *et al.*, 2008 *JCAP* **0810** 018 [arXiv:0807.4730 [astro-ph]]
[9] Castellina A and Donato F, 2005 *Astropart. Phys.* **24** 146 [arXiv:astro-ph/0504149]
[10] Ahn H S *et al.* [CREAM collaboration], 2008 *Astropart. Phys.* **30** 133 [arXiv:0808.1718 [astro-ph]]
[11] Adriani O *et al.*, [PAMELA collaboration], 2009 *Phys. Rev. Lett.* **102** 051101 [arXiv:0810.4994 [astro-ph]]
[12] Blasi P and Serpico P D, 2009 *Phys. Rev. Lett.* **103** 081103 [arXiv:0904.0871 [astro-ph.HE]]
[13] Blasi P, 2009 *Phys. Rev. Lett.* **103** 051104 [arXiv:0903.2794 [astro-ph.HE]]
[14] Bergstrom L, Edsjo J and Ullio P, 1999 *Astrophys. J.* **526** 215 [arXiv:astro-ph/9902012]
[15] Bergstrom L *et al.*, 2009 *Phys. Rev.* **D79** 081303 [arXiv:0812.3895 [astro-ph]]
[16] Bertone G *et al.*, 2009 *JCAP* **0903** 009 [arXiv:0811.3744 [astro-ph]]
[17] Cirelli M, 2009 *Nucl. Phys.* **B813** 1 [arXiv:0809.2409 [hep-ph]]
[18] Moskalenko I V *et al.*, 2002 *Astrophys. J.* **565** 280 [arXiv:astro-ph/0106567]
[19] Donato F *et al.*, 2001 *Astrophys. J.* **536** 172 [arXiv:astro-ph/0103150]
[20] Ginzburg V L and Syrovatskii S I, 1964 "The Origin of Cosmic Rays", New York, MacMillan
[21] Ferrière K M, 2001 *Rev. of Mod. Phys.* **73** 1031 [arXiv:astro-ph/0106359]
[22] Evoli C, Grasso D and Maccione L, 2007 *JCAP* **0706** 003 [arXiv:astro-ph/0701856]
[23] Strong A W *et al.*, 2004 *Astron. Astrophys.* **422** L47 [arXiv:astro-ph/0405275]
[24] Maestro P *et al.*, 2009 [CREAM Collaboration], Proc. of the 31st International Cosmic Rays Conference, Lodz, Poland
[25] Boyle P J [TRACER Collaboration], 2008 *Mod. Phys. Lett.* **A23** 2031 [arXiv:0810.2967 [astro-ph]]
[26] Ave M et al. [TRACER Collaboration], 2009 *Astrophys. J.* **697** 106 [arXiv:0810.2972 [astro-ph]]
[27] Sanuki T *et al.* [BESS Collaboration], 2000, Astrophys. J. **545** 1135 [arXiv:astro-ph/0002481]
[28] Aguilar M *et al.* [AMS-01 Collaboration], 2002 *Phys. Rept.* **366** 331; Erratum-ibid. 2003 **380** 97
[29] We extracted this data from the slides of the talk of P. Picozza at the TeVPA 2009 conference, under permission of the author, http://www-conf.slac.stanford.edu/tevpa09/Talks.asp
[30] Letaw J R, Silberberg R and Tsao C H, 1983 *Astrophys. J. Supp.* **51** 271; 1984 *Astrophys. J. Supp.* **56** 369
[31] Webber W R, Kish J C and Schrier D A, 1990 *Phys. Rev.* **C41** 520
[32] Silbeberg R and Tsao C H, 1990 *Phys. Rep.* **191** 351
[33] Tan L C and Ng L K, 1982 *Phys. Rev.* **D26** 1179; 1983 *J. Phys.* **G9** 227
[34] Asplund M, Grevesse N and Sauval J, 2006 *Nucl. Phys.* **A777** 1 [arXiv:astro-ph/0410214]
[35] Gleeson L J and Axford W I, 1968 *Astrophys. J.* **154** 1011
[36] George J S, 2009 Astrophys. J. **698** 1666; ACE website http://www.srl.caltech.edu/ACE/ASC/DATA/level3/cris/CRISminmax_spectra.txt
[37] Meyer J P, 1985 Astrophys. J. **S57** 173
[38] Binns W R *et al.* [HEAO-3 Collaboration], 1989 *Astrophys. J.* **346** 997
[39] Tomassetti N [AMS-01 Collaboration], 2009 Proc. of the 31st International Cosmic Rays Conference, Lodz, Poland
[40] Swordy P S *et al.*, 1990 *Astrophys. J.* **349** 625
[41] Boezio M et al. [WiZard/CAPRICE Collaboration], 2001 *Astrophys. J.* **561** 787 [arXiv:astro-ph/0103513]
[42] Ptuskin V. S. et al., 2006 *Astrophys. J.* **642** 902 [arXiv:astro-ph/0510335]

[43] Blasi P, 2007 Proc. of the 30th International Cosmic Ray Conference, Merida, Mexico, **6** 279 [arXiv:0801.4534 [astro-ph]]

[44] S. Rosier-Lees [AMS-02 Collaboration], 2007 Proc. 30th International Cosmic Ray Conference, Merida, Mexico, **4** 729